

Testing the X-ray variability of active galactic nuclei with the nonlinear prediction method

Bożena Czerny

Nicolaus Copernicus Astronomical Center, Bartycka 18, 00-716 Warsaw, Poland; e-mail: bcz@camk.edu.pl

Harry J. Lehto

Turku University Observatory, Tuorla, Väisäläntie 20, FI- 21500 Piikkiö, Finland; e-mail: hlehto@astro.utu.fi

ABSTRACT

The analysis of eight EXOSAT X-ray lightcurves of six active galactic nuclei by nonlinear prediction methods indicates that the observed variability is truly stochastic and is not caused by deterministic chaos. This result favors X-ray emission models with multiple centers of production of hot, possibly relativistic electrons.

Key words: galaxies: Seyfert - X-rays: galaxies - chaotic phenomena

1 INTRODUCTION

X-ray emission is clearly one of the key points in understanding the nature of radio quiet AGNs. It comprises a substantial fraction of the total bolometric luminosity and is strongly variable on time scales as short as hours (see, e.g. Mushotzky, Done & Pounds 1993). Any AGN model must therefore explain both the level of X-ray emission and its rapid variability.

The longest (up to 2×10^5 s) uninterrupted light curves for short time scale variability studies in the 1–8 keV range have been provided by the EXOSAT due to its unusual orbit. Longer time scale variability has been studied by combining data from different satellites over several years.

Several characteristics of X-ray variability of AGN have emerged in these studies. The X-ray flux is strongly variable (e.g. McHardy 1988, Green, McHardy & Lehto 1993) in most sources. Power spectra are featureless and have a power-law shape $S \propto \nu^\alpha$, with $\alpha \sim -1$ over a broad range of frequencies ($\sim 10^{-5} - 10^{-3}$ Hz) (McHardy & Czerny 1987, Lawrence et al. 1987, Lehto et al. 1991; for a review see, e.g. McHardy 1990). The only features seen in these spectra are the expected flattening of the spectrum at timescales of years, which is claimed for NGC 5506, and the signs of quasi-periodicity in NGC 5548 (Papadakis & Lawrence, 1993) and NGC 4051 (Papadakis & Lawrence, 1995). Note that the claimed periodicity in NGC 6814 (Mittaz & Branduardi-Raymont 1989; Done et al. 1992) was subsequently discovered to be the property of the galactic X-ray source contaminating the X-ray measurements in the direction of this AGN (Madejski et al. 1993).

As the primary emission strongly dominates in the EXOSAT energy range we can assume that the conclusions apply directly to the primary power-law component of the X-ray emission.

An observed featureless power spectrum is expected in two qualitatively different dynamical systems:

(A) a system consists of a large number of uncorrelated (weakly correlated) elements varying (almost) independently

(B) global evolution of the system is described by three or more non-linear differential equations which shows deterministic chaos behaviour.

These two interpretations lead to two different physical pictures.

Case (A) can be interpreted, for example, as randomly generated shocks in outflowing (or accreting) gas, or randomly appearing reconnections of large scale magnetic field lines, in close analogy to phenomena in solar corona. In this case the emitting medium is clearly clumpy and the emission itself can be modelled as a shot noise (e.g. Lehto 1989).

Case (B) could correspond to coherent variability of a single cloud of electrons, e.g. some generalization of optically thin geometrically thick disk, spherically accreting hot (possibly pair dominated) plasma or instability of a single shock at the base of jet forming region.

Sugihara & May (1990) suggested that nonlinear prediction methods are (in principle) capable of distinguishing between cases (A) or (B).

The methods (Tsonis & Elsner 1992) are based on the study of the decay of short term correlations in the light curve. Exponential decay of the correlation is characteristic for a chaotic signal with a strange attractor while a power law decay is expected from shot noise (more precisely, from the so called fractional brownian motion representing stochastic phenomena with power law power spectra).

We apply this new method to a number of long EXOSAT observations of Seyfert galaxies to which the correlation integral method has been applied previously by Lehto, Czerny & McHardy (1993; hereafter LCMH).

2 METHOD

We apply the non-linear prediction methods of Tsonis and Elsner (1992) to investigate the characteristics of X-ray variability of several AGNs that show broadband $1/f^\alpha$ type power spectra. The essence in these methods is to break up the data into short strings of consecutive data points and then to analyse the statistical properties of these strings. They are far more efficient than the Fourier methods in studying the behaviour of a system with short term correlations.

The method compares shapes of two data strings of length d . Mathematical expression of that procedure is the calculation of the distance between the two strings, or vectors $X = (x_1, x_2, \dots, x_d)$ and $Y = (y_1, y_2, \dots, y_d)$. Usually the distance r , or the norm, is defined as the L_2 norm of the difference vector:

$$r = \left(\sum_{i=1,d} (x_i - y_i)^2 \right)^{\frac{1}{2}}, \quad (1)$$

in close analogy to χ^2 fit of two curves. We adopt this definition in our paper. Other norms can also be used, for example, the Chebychev or L_∞ norm,

$$r^* = \max_{i=1,d} (|x_i - y_i|). \quad (2)$$

The aim of the nonlinear prediction method is used in an attempt to predict the position of the point separated by time interval T from the sequence Y on the basis of known library data set X_K .

This consists of three steps: (i) identifying the sequences from the library $\{X_K\}$ most similar to the one being considered (Y) (by minimizing the norm between) (ii) identifying values the strings in the library would get after a timestep T (iii) calculating the predicted value using the values from (ii) (iv) and finally correlating it with the observed value.

We have used three different methods for step (iii):

- *Nearest Point Method.* Identify the nearest X as the best predictor sequence. Use that sequence alone to predict Y after at time interval T .
- *Linear Interpolation Method.* Identify the $d + 1$ closest sequences. Use linear interpolation in d dimensional space to obtain a predicted value after a time interval T from the predictor sequences.
- *Exponential Weight Method.* Identify $d + 1$ closest sequences. Predict Y at time interval T by using the observed values of the X sequences, but now interpolating them with a weight of $\exp(-r)$ for each predictor value, where r is the distance between the given sequence and Y .

We divide the data sequence into two halves. The first part forms the library and the second one is used to test the quality of prediction. Since we actually know the values, we have a set of pairs (p_k, f_k) consisting of the predicted and known value for step (iv).

The quality of prediction can be evaluated by calculating the correlation coefficient R between the series of predicted p_k and known f_k values:

$$R(T) = (\langle p_k f_k \rangle - \langle p_k \rangle \langle f_k \rangle) / \sigma^2 \quad (3)$$

where $\langle \cdot \rangle$ denote the average of the quantity over the series and σ , the standard deviation of the mean value of the time series.

If the data is dominated by short term correlations the quality of prediction decreases with time step T . Tsonis & Elsner (1992) shows that for, for chaotic signal (in a sense of deterministic chaos)

$$1 - R(T) \propto \exp(2KT) \quad (4)$$

and in the case of fractal brownian motion (shot noise)

$$1 - R(T) \propto T^{2H} \quad (5)$$

Here K is the Kolmogorov entropy (Kolmogorov 1959) which is the sum of the positive Lyapunov exponents (see e.g. Schuster 1989) and H is related to the slope a of the power density spectrum through the relation $a = 2H + 1$.

By correlating $\log(1 - R)$ against T and against $\log(T)$ we obtain R_d and R_s , two further correlation coefficients which tell us how well each of the two predictive models describes the data. We identify the preferred system by selecting the system with the larger of R_s and R_d .

3 RESULTS

3.1 Tests of the method using NGC 4051 ME

We tested technical details such as the choice of length string, d , the binning, the method of prediction and the time range of prediction on the EXOSAT ME X-ray lightcurve of NGC 4051.

Binning the data is the standard approach to increase the signal to noise ratio. This is done at an expense of the available dynamical range.

We used generally 200 second bins, corresponding to S/N ratio of 6 in NGC 4051. We made also some further tests with 50 second bins.

The value of the correlation coefficient depends on the assumed length of the string d . Therefore we first calculated this coefficient for d ranging from 1 to 20 and the prediction time step $T = 1$ (one bin). We show this dependence in fig.1 using the three different prediction methods. The linear interpolation method was used only up to $d = 4$, as the search for the smallest simplex containing a given vector (c.f. Sugihara and May 1990) is time consuming.

We can see that the third method, i.e. the exponential weight gives the highest values of the correlation coefficient and relatively small wiggles around the systematic trend. Therefore, in all the following computations, we use the exponential weight method to compute the predicted values.

The value d_{max} corresponding to the best prediction is picked up for the purpose of further calculations for larger T .

We also tested the prediction for the same time interval (i.e. 200 s) but with bins of 50 seconds. The highest values for the correlation coefficient were met for strings approximately longer by a factor 4, as expected, but the values of the correlation coefficient was lower. It was also lower for the prediction for a single time step (i.e. 50 s). Too strong binning will lead to a loss of information about the correlations in the system. Assuming time step 800 s (binning

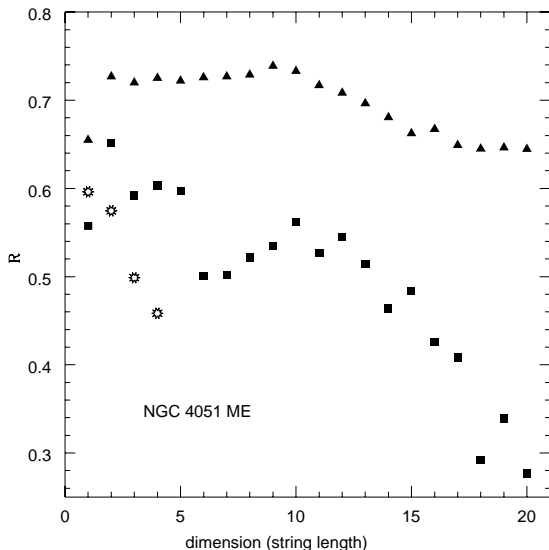


Figure 1. The dependence of the correlation coefficient on dimension of the string used for prediction. NGC 4051 ME light curve is used as an example. Prediction time step equal 1 bin (200 s). Three prediction methods were used: nearest point (squares), linear interpolation (stars) and exponential weight (triangles).

again by a factor 4) results also in the decrease of the correlation coefficient of the prediction for a single time step (i.e. 800 s). Our initial 200 second binning appears therefore reasonable.

Next we calculate the prediction quality as a function of prediction time. We use 200 second bins and strings of 9 points. Figure 2 shows the result of plotting $\log(1 - R)$ vs. $\log(T)$ and $\log(1 - R)$ vs. T .

The distinction between the two cases is not very profound, but a clear tendency is seen to favor the log-log dependence, which corresponds to the fractal brownian type shot noise variability. The correlation coefficient R_s is 0.998, and the coefficient R_d is equal 0.958.

We test the dependence of the measured correlation decay on the choice of the string length. In Fig. 3 we show the same plot as in Fig 2b but derived using different string length d_{max} . We see that for the string length $d_{max} = 9$ the plot is very smooth whilst shorter length values introduce more wiggling. However, in all cases the correlation coefficient R_s is greater than R_d and the slopes of the curves are similar. Therefore the use of the string length giving the best prediction for a single time step seems to be well justified.

We may be tempted to obtain more significant result by increasing the dynamical range of the study, that is making predictions for even longer time steps. However, the decay of correlations takes us into the range dominated by the data noise after some 15 steps, i.e. interval of 3000 seconds for this source.

Since the shot noise is favored the slope, $2H$, of the curve $\log(1-R)$ vs. $\log(T)$ should be related to the slope of the power spectrum, a , through the relation $a = 2H + 1$. As $2H = 0.42$ and the power spectrum slope determined by Papadakis & Lawrence (1995) for this lightcurve is $a = 1.46^{+0.10}_{-0.05}$, the two numbers are in agreement.

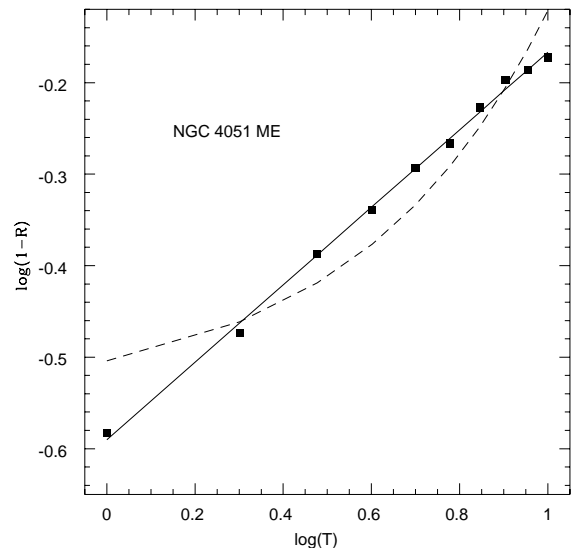
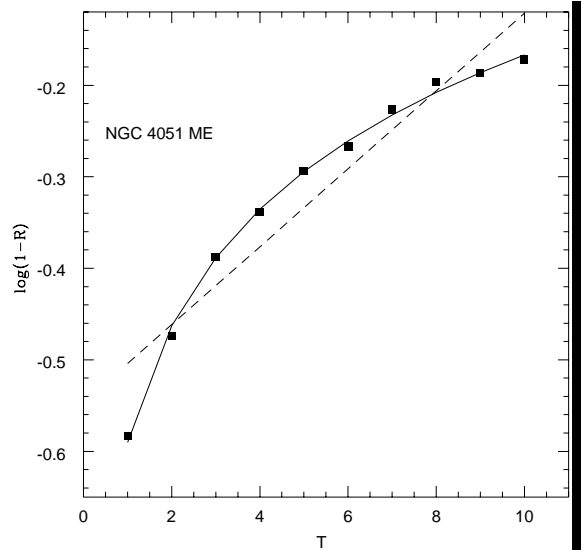


Figure 2. The quality of prediction (see eq. 4 and 5) as a function prediction time step for exponential method. The decay of correlation, i.e. decrease of R is clearly visible. The rate of this decay is better represented by a straight line on plot $\log(1-R)$ vs. $\log(T)$ (lower panel) than $\log(1-R)$ vs. T (upper panel). Best power-law fit to the decay law is shown with continuous line whilst best exponential fit to decay is shown with dashed line on both panels. The respective correlation coefficients for these fits R_s and R_d are equal to 0.998 and 0.958, thus stochastic interpretation of the lightcurves is clearly favored.

3.2 Simulated lightcurves

In order to test the sensitivity of the method we use two computer generated light curves of the equal lengths. The first one is the Lorenz attractor (Lorenz 1963), an example of a source exhibiting deterministic chaos. We use a time step 0.02 and the coordinate X to represent the light curve as in our previous paper (LCMH). The correlation decay plot for this lightcurve is shown in Fig. 4.

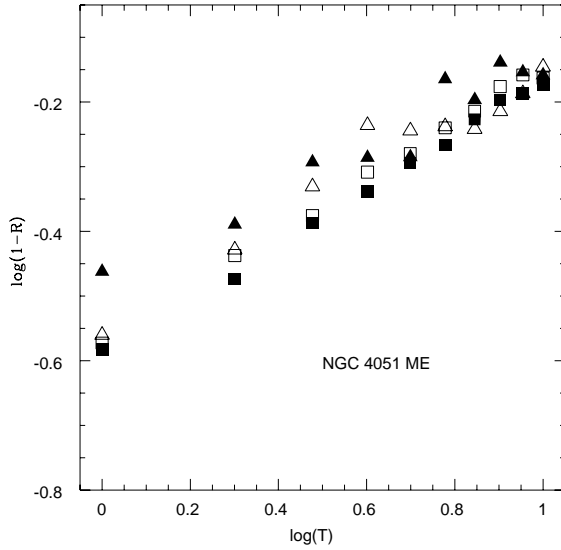


Figure 3. The dependence of the quality of prediction on the adopted length of the string. The values used are: 1 (filled triangles), 4 (open triangles), 9 (filled squares) and 10 (open squares). All values favour stochastic interpretation of the lightcurve. The value 9, giving the highest correlation in prediction for a single step is adopted in further computations for this lightcurve.

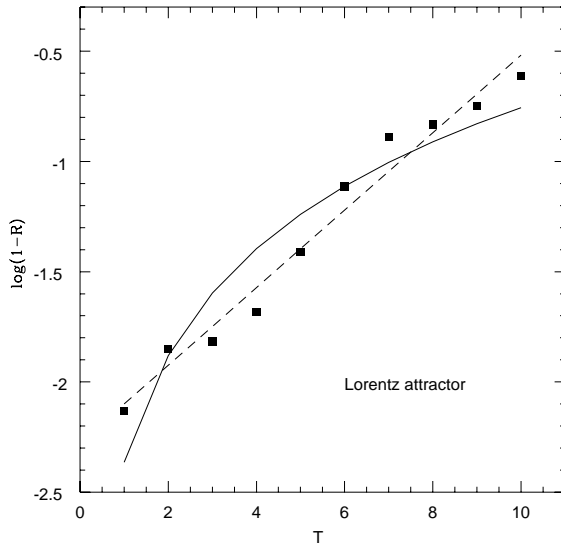


Figure 4. The decay of correlations as a function of prediction time step for a simulated light curve formed from the X-coordinate of the Lorenz attractor. Exponential decay (dashed line) is favored (see eq. 4) over the power law trend (continuous line). This is expected because this case is an example of a simulated light curve caused by deterministic chaos.

As expected, the character of variability is better described by exponential decay of correlations, and the coefficient R_s is smaller than R_d (0.949 and 0.986 respectively, for the length of lightcurve 2000 points).

The second computer generated lightcurve is an example of shot noise (Lehto 1989). Again, the nonlinear predic-

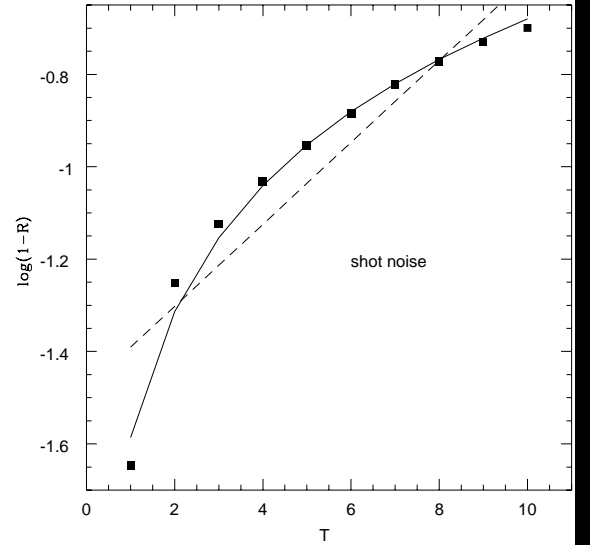


Figure 5. The decay of correlations as a function of prediction time step for computer generated example of stochastic light curve; as expected, this time power law trend (continuous line) is favored (see eq. 5) over the exponential law (dashed line).

tion method unveils correctly the nature of the light curve ($R_s = 0.99$, $R_d = 0.92$).

3.3 EXOSAT background

The effects of background subtraction may, in principle, influence the results of a variability study (see e.g. Fiore & Massaro 1989). Fig. 6a shows the decay of correlations for NGC 4051 ME lightcurve (background subtracted) and the background itself. Clearly the behaviour of the two is different. The level of correlations in the background is quite high and it almost does not decay with the increase of the prediction time. The formal fit slightly favors the interpretation of deterministic chaos, as the R_d and R_s coefficients for the ME background during the observation of NGC 4051 are equal to 0.904 and 0.878, respectively. Such long range correlations may reflect some systematic trends of unknown nature. However, it is encouraging, that correlations present in the signal are markedly different from those present in the background.

In the case of LE EXOSAT lightcurve of NGC 4051 (Fig. 6b), the decay of correlations for the source is smooth and nicely follows a straight line on log-log diagram; the behaviour of the background is badly approximated by any of the two laws. It shows again that the correlations are not just artifacts of the background subtraction but the real property of the source.

3.4 EXOSAT lightcurves

The nonlinear prediction method was applied to a number of long EXOSAT X-ray lightcurves. The data was binned in 200 s. The exponential weight method was used for prediction. We excluded the light curve of NGC 6814 because it is strongly contaminated by the X-ray emission from a variable galactic source (Madejski et al. 1993).

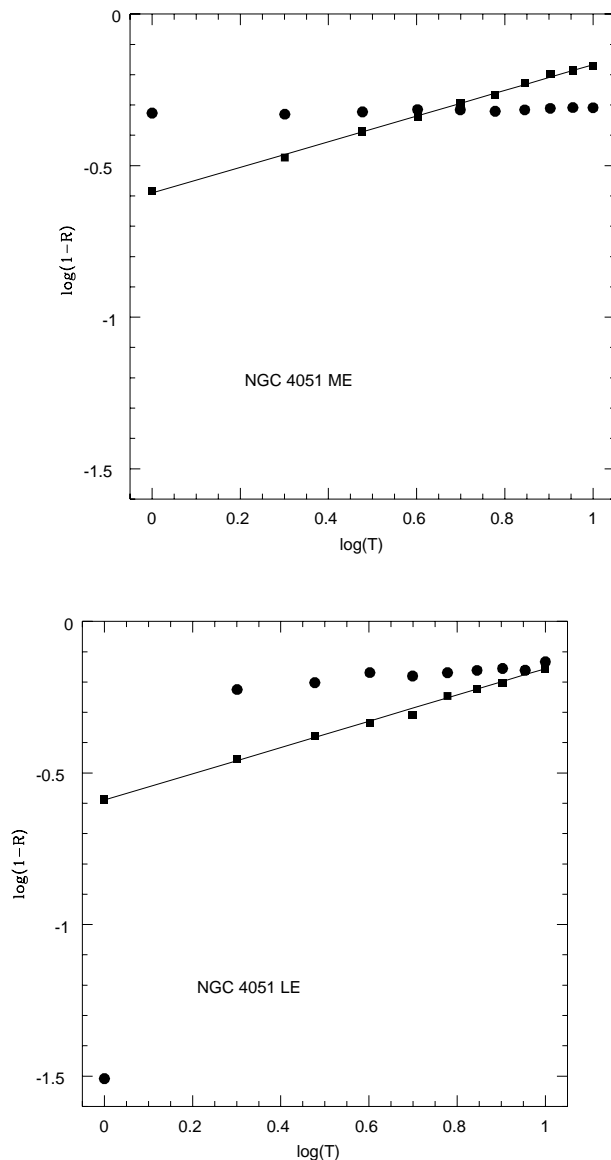


Figure 6. The decay of correlations as a function of prediction time step for the source lightcurve (NGC 4051) (squares) and the background (circles) from the two EXOSAT instruments: ME (upper panel) and LE (lower panel). Straight lines show the best fit to the decay of correlations under the assumption of the stochastic nature of the signal.

Seven light curves are from EXOSAT ME instrument sensitive to 1 - 8 keV radiation. One lightcurve of NGC 4051 is from EXOSAT LE instrument operating in 0.25 keV - 1.5 keV band.

The correlation coefficients R_s , R_d of the light curves are shown in Table 1 with some other relevant information.

The correlation coefficients of the light curves appear to fall into two classes. The same separation is also evident if plotting the decay of prediction quality as a function of adopted time step.

Class 1 contains Mkn 335, NGC 4151 and 3C 273. All these sources are characterized by rather low values ($|R| \leq 0.2$) of both correlation coefficients for time steps greater

Table 1. The correlation coefficients for power law and exponential decay of correlations in EXOSAT lightcurves.

Name	Obs.time(10^3 s)	R_d	R_s	Class
Mkn335	67	0.557	0.562	1
NGC4151(93)	62	0.580	0.753	1
NGC4151(95)	37	0.544	0.741	1
3C273	142	0.557	0.750	1
MCG6-30-15	178	0.977	0.993	2
NGC5506	239	0.947	0.984	2
NGC4051 _{LE}	202	0.843	0.959	2
NGC4051 _{ME}	196	0.954	0.999	2

than 1 bin although the prediction for one bin is sometimes significant - the same effect is observed in the behaviour of the background lightcurve (see Sec. 3.2). Visually the four light curves appear to show little variation on short timescales. On timescales of hours slowly varying trends are apparent.

No conclusion on the character of variability in these sources can be drawn on formally fitted coefficients R_s and R_d , which are not significant (lower than ~ 0.8). The ratio of the two coefficients is in all four light curves is greater than 1, which may favor stochastic behaviour. However, the same is true for the background lightcurve. It appears that the low correlation coefficients can be understood as being caused by the dominance of poisson noise to real variability of the source on short timescales.

Class 2 contains NGC 4051 (both ME and LE), MCG 6-30-15 and NGC 5506. All these sources show a range of prediction time steps with high prediction quality and the decay of prediction quality is smooth. The correlation coefficients R_s and R_d are highly significant, and the ratio is larger than 1.

This result means that (at least in class 2 sources) the variability is caused by a truly stochastic phenomenon and not by the deterministic chaos.

The nonlinear prediction method used in this paper is basically different from the correlation integral method used to these sources in our previous paper (LCMH). Therefore it is interesting to note that the classification of the sources proposed by us has not changed much. Class 1 sources from LCMH (white noise) all found their place in a new class 1 (sources without good description of short term correlations). A source classified as class 2b in LCMH (NGC 4151) moved to a new class 1. All old class 2 sources (shot-noise type behaviour) are again in class 2 and the stochastic character of their variability found a strong support from the nonlinear prediction method.

The key result is that the lightcurve NGC 4051_{LE} suspected of chaotic behaviour on the basis of the correlation integral method now revealed itself as just another stochastic phenomenon.

It is also interesting to note that the character of variability of the source NGC 4051 in LE and ME band is very similar, the slopes, $2H$, for the two lightcurves are equal 0.43 and 0.42, correspondingly, as if the (at least variable fraction of) radiation comes from the same region and the same emission mechanism. This conclusion was by no means obvious as in many Seyfert galaxies the soft X-ray band is dominated by the soft X-ray excess and the presence of an

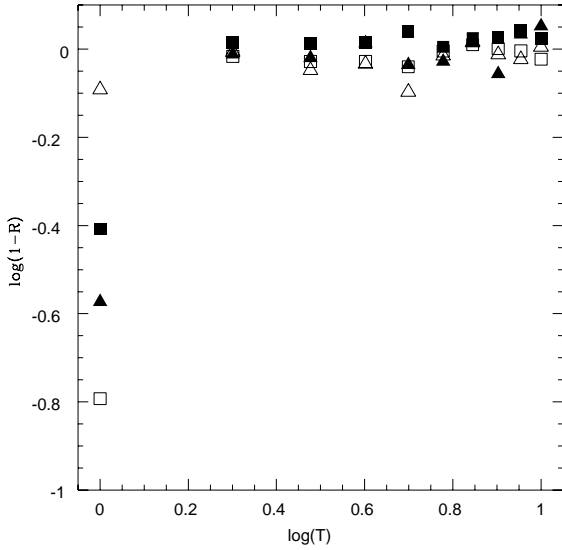


Figure 7. The decay of correlations as a function of the prediction time step for sources from the Class 1: filled squares - 3C273, filled triangles - NGC 4151 in 1983, open squares - NGC 4151 in 1985, and open triangles - Mkn335.

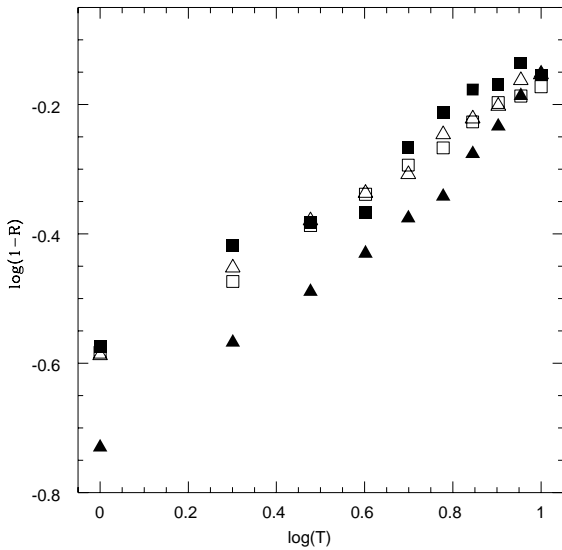


Figure 8. The decay of correlations as a function of the prediction time step for sources from the Class 2: filled squares - NGC 5506, filled triangles - MCG 6-30-15, open squares - NGC 4051_{ME}, open triangles - NGC 4051_{LE}

excess, albeit not a strong one, was also invoked in the case of NGC 4051 (e.g. Walter & Fink 1993).

What is more, the slope of the power spectrum of LE curve calculated by Papadakis and Lawrence (1995) is significantly steeper than that of ME curve. On the other hand the conclusion of their paper was that power law is not a good representation of the power spectrum of LE curve. Visual inspection of their Fig. 10 shows that if a single point at $\log(\nu) \sim -4.2$ is removed the mean slope would be again consistent with the ME slope and with our result. Perhaps

there is an additional power at around this frequency as well. An extension of the power spectrum towards longer timescales based on combined observations on a number of satellites operating recently might give the answer.

4 DISCUSSION

4.1 Deterministic chaos vs. stochastic signal

A number of works have been already devoted to the search of low-dimensional chaos in different astronomical objects, e.g. Voges, Atmanspacher & Scheingraber (1987), McHardy & Czerny (1987), Canizzo & Goodings (1988), Lochner, Swank & Szymkowiak (1989), Norris & Matilsky (1989), Fiore & Massaro (1989), Cannizzo, Goodings & Mattei (1990), Harding, Shinbrot & Cordes (1990), Kollath (1990), Krolik, Done & Madejski (1993), LCMH.

However, the methods used do not provide the unique answer to the question unless they are supplemented by methods sensitive to the difference between low-dimensional deterministic chaos and stochastic phenomenon. One such method (nonlinear prediction test of Tsonis & Elsner 1992) was applied in this paper whilst two other methods (phase randomization method of Theiler 1992 and signal differentiation method of Provenzale et al. 1992) were used for analysis of the optical lightcurve of quasar 3C 345 by Provenzale, Vio & Cristiani (1994).

In both cases the tests indicated stochastic nature of the astronomical phenomenon. This shows clearly the importance of the supplementary tests; any reliable claims of deterministic chaos have to pass at least one such test.

4.2 Consistency of the thermal Comptonization model of X-ray emission with the observed variability

On the basis of their results on the variability of NGC 4051 Papadakis & Lawrence (1995) concluded that thermal Comptonization models are ruled out since they always predict steeper ME spectra than LE spectra whilst the observations give the opposite effect. Since the thermal Comptonization is currently the most popular mechanism (see e.g. Zdziarski et al. 1995) we rediscuss this conclusion within the light of our results.

Since the correlation slope, $2H$, calculated for the ME and LE curve (see Section 3.4) are the same our conclusion is that the character of variability (and the mean slopes of the power spectra) are actually the same for both lightcurves. In the light of Compton scattering model it implies that the multiple travel time within the hot plasma is shorter than the timescale for variations of the plasma parameters.

As the mean energy photon in LE band is 0.2 keV and it is 4 keV in ME band (Papadakis & Lawrence 1995) the energy change of the photon by a factor 20 is required to change LE photon into ME one. The relative energy change is a single scattering is approximately given by

$$\frac{\Delta\epsilon}{\epsilon} = \Theta(1 + \Theta); \quad \Theta = \frac{4kT_e}{m_e c^2}, \quad (6)$$

where T_e is the electron temperature of the thermal plasma. The number n of scattering required to interchange LE into ME photon can be therefore estimated from the relation

$$\left(\frac{\Delta\epsilon}{\epsilon}\right)^n = 20. \quad (7)$$

This number is about 8 if the temperature of the plasma is ~ 100 keV and only about 2 if it is ~ 200 keV.

Therefore, if the plasma temperature is high, the measured delay does not have to be much smaller than a factor few times the light travel time of the emitting region and the lack of noticeable delay between the LE and ME lightcurves of NGC 4051 (< 60 s, Papadakis & Lawrence 1995) simply translates into the size of the emitting region of order of a fraction of a Schwarzschild radius adopting the value of the mass of the central black hole equal $7 \times 10^6 M_\odot$.

It may well be consistent with the models of relatively flat corona, the height being a fraction of the radius and the emissivity strongly peaked close to the horizon of the black hole. Exceptionally detailed studies of the K_α iron line in Seyfert galaxy MCG 6-30-15 (Iwasawa et al. 1996) supports similar view, which also strongly suggests that the central black hole is rapidly rotating.

4.3 Constraints for stochastic models from the power spectra

The conclusion from the analysis of the character of X-ray light curves of (predominantly) radio-quiet AGN can be applied to the detailed models of the X-ray emission.

The stochastic nature of variability of X-ray radiation from active galactic nuclei well agrees with the coronal nature of emission proposed by Galeev, Rosner & Vayana (1979); De Vries & Kuipers (1992); Haardt, Maraschi & Ghisellini (1994); Stern et al. (1995).

For example, in the solar corona the energy is stored in a form of magnetic field loops, and then released during reconnections which results in an event of solar flare (see e.g. Demoulin et al. 1993). The efficiency of X-ray production is not very high in this case: only some 10% of the flare energy is emitted in the form of X-ray radiation (Confield et al. 1980). However, the strength of the magnetic field in an accretion disk may be considerably higher as the rotational velocity is very high (Keplerian) and field amplification may operate far more efficiently.

The stochastic nature of the variability does not prove that the magnetic field growing in the result of dynamo action within the disk is the original cause of the variability, as some corona models were assumed to be powered by coronal accretion itself (e.g. Życki et al. 1995, Witt et al. 1996) and any instabilities growing within such a corona would give basically similar effect.

Unfortunately, most of the models deal mostly with the stationary solutions (frequently at a single representative radius) and the attention is focused on the radiation spectra so at present it is impossible to say whether these models are consistent with the variability studies.

The only model, which can be directly tested against the time dependent properties is the clumpy corona model developed by Haardt, Maraschi & Ghisellini (1994).

In the model of Haardt et al. (1994) the evolution of a single clump consists of two phases. The first phase, invisible and much longer, is the charge time when the energy accumulates within a clump due to magnetic field. The second phase is the rapid discharge accompanied with a flash of radiation. The charge time in this model depends on the radial position of the formed clump ($t_C \sim r^{5/2}$) whilst the discharge time is independent from radius. Therefore the

set of shots consist of the shots with a range of amplitudes ($I_{blob} \sim r^{1/2}$) and the same decay times. The power spectra of such a shot noise are given by a formula (Lehto 1989, Papoulis 1984)

$$F(\omega) = 2\pi\lambda^2 t_d^2 \delta(\omega) + \frac{\lambda}{\omega^2 + 1/t_d^2}, \quad (7)$$

where $1/\lambda$ is the average time interval between shots. Such a power spectrum has a shape strongly different from a power law with the slope ~ 1.5 . More complex coupling between the matter and the magnetic field has to be invoked to get an agreement with the observed power spectra.

4.4 Future observations

The method of timeseries analysis presented in this paper could be improved by longer data streams (several thousand points) and a low signal to noise ($S/N \sim 1$). The contiguous sections of the data should last at least a time $\sim 10 - 20$ times longer than the separation of two significant data points.

5 CONCLUSIONS

The nonlinear prediction method applied to the EXOSAT X-ray lightcurves of Seyfert galaxies indicates that

- (i) there are no signs of the deterministic chaos in the analyzed X-ray lightcurves of the Seyfert galaxies
- (ii) in four out of eight cases the signal is clearly of stochastic nature thus generally supporting emission models based on multiple active centers
- (iii) in the remaining four cases the variability is not strong enough to determine reliably its character but again the stochastic interpretation is favored.

These conclusions apply to the short term variability, with the timescales covering from ~ 200 s to ~ 4000 s. Long timescale phenomena, lasting months - years, may be of different nature as the overall spectral changes accompanying large UV brightenings observed in some sources are distinct from those observed during the short timescale variation (e.g. Done et al. 1995 for NGC 5548; Clavel, Wamsteker and Glass 1989 for Fairall 9).

ACKNOWLEDGMENTS

We are deeply grateful to Ian McHardy for many helpful discussions, as well as for providing us with the extracted background lightcurves used in Section 3.3. We also want to acknowledge the considerable help of Piotr Życki in formulating the numerical scheme for the search of the simplexes necessary for the use of linear interpolation method. We thank Andrzej Zdziarski and Andy Lawrence, the referee, for very helpful comments on the original version of the manuscript. This project was partially supported by the grants nos. 2P 304 01004 and 2P 03D 00410 of the Polish State Committee for Scientific Research.

REFERENCES

- Arnaud, K.A., et al. 1995, MNRAS, 217, 105
- Bregman, J., 1994, in Multi-wavelength continuum emission of AGN, eds. T. Courvoisier & A. Blecha, Kluwer Academic

- Publishers, p. 5
- Canizzo, J.K., Goodings, D.A., 1988, *ApJ*, 334, L31
- Canizzo, J.K., Goodings, D.A., Mattei, J.A., 1990, *ApJ*, 357, 235
- Clavel, J., Wamsteker, W., Glass, I.S., 1989, *ApJ*, 337, 236
- Confield et al., 1980, ed. P.A. Sturrock, *Solar Flares*, Colorado Associated University Press, Boulder, p. 231
- Czerny, B., Życki, P.T., Loska, Z., 1995, in *Proceedings of 17th Texas Symposium on Relativistic Astrophysics* (in press)
- Czerny, B., 1994, in *Multi-wavelength continuum emission of AGN*, eds. T. Courvoisier & A. Blecha, Kluwer Academic Publishers, p. 261
- Demoulin P., van Driel-Gesztelyi L., Schmieder R., Henoux J.C., Gsepura C., Hagyard M.J., 1993, *A&A*, 271, 292
- de Vries, M., Kuipers, J., 1992, *A&A*, 266, 77
- Done, C. et al., 1992, *ApJ*, 400, 138
- Done, C., Pounds, K.A., Nandra, K., Fabian, A.C., 1995, *MNRAS*, 275, 417
- Fabian, A.C., et al., 1994, *PASJ*, 46, L59
- Fiore F., Massaro E., 1989, ed. G. Belvedere, *Accretion Disks and Magnetic Fields in Astrophysics*, Kluwer Academic Publishers, p. 267
- Galeev A.A., Rosner R., Vayana G.S., 1979, *ApJ*, 229, 318
- Green, A.R., McHardy, I.M., Lehto, H.J., 1993, *MNRAS*, 265, 664
- Haardt, F., Maraschi, L., 1991, *ApJ*, 380, L51
- Haardt, F., Maraschi, L. & Ghisellini, G., 1994, *ApJ*, 432, L95
- Harding, A.K., Shinbrot, T., Cordes, J.M., 1990, *ApJ*, 353, 588
- Iwasawa, K. et al. 1996, *MNRAS* (in press)
- Kolath, Z., 1990, *MNRAS*, 247, 377
- Kolmogorov A.N., 1959, *Dokl. Acad. SSSR*, 124, 754
- Krolik, J., Done, C., Madejski, G., 1993, *ApJ*, 402, 432
- Lawrence, A., Pounds, K.A., Watson, M.G., Elvis, M.S., 1987, *Nat.*, 325, 692
- Lehto, H.J., 1989, in Hunt J., Battrick B., eds, *Proc. 23rd ESLAB Symp., Two Topics in X-ray Astronomy*, ESA, Noordwijk, p. 499
- Lehto, H.J., McHardy, I.M., Abraham, R.G., 1991, in Miller, R., Wiita P.J., eds, *Variability of Active Galactic Nuclei*, Cambridge Univ Press p. 256.
- Lehto, H.J., Czerny, B., McHardy, I.M., 1993, 261, 125 (*LCMH*)
- Liang, E.P., Price, R.H., 1977, *ApJ*, 217, 247
- Lightman, A.P., White, T.R., 1988, *ApJ*, 335, 57
- Lochner, J.C., Swank, J.H., Szymkowiak, A.E., 1989, *ApJ*, 337, 823
- Lorenz, E.N., 1963, *J. Atmosph. Sci.*, 20, 130
- Madejski, G.M., Done, C., Turner, T.J., Mushotzky, R.F., Serlemitsos, P., Fiore, F., Sikora, M. & Begelman, M.C., 1993, *Nat.*, 365, 626
- Masnou, J.P., Wilkes, B.J., Elvis, M., McDowell, J.C., Arnaud, K.A., 1992, *A&A*, 253, 35
- Matsuoka, M., Yamauchi, M., Piro, L., Murakami, T., 1990, *ApJ*, 361, 440
- Mittaz, J.P.D., Branduardi-Raymont, G., 1989, *MNRAS*, 238, 1029
- McHardy, I.M., 1988, *Mem. S. A. It.*, 59, 239
- McHardy, I.M., 1989, in Hunt J., Battrick B., eds, *Proc. 23rd ESLAB Symp., Two Topics in X-ray Astronomy*, ESA, Noordwijk, p. 1111
- McHardy, I.M., Czerny, B., 1987, *Nat.*, 325, 696
- Mushotzky, R.F., Done, C., Pounds, K.A., 1993, *ARAA*, 31, 717
- Nandra, K., Pounds, K.A., 1994, *MNRAS*, 268, 405
- Nandra, P., Pounds, K.A., 1992, *Nat.*, 359, 215
- Netzer, H., 1993, *ApJ*, 411, 594
- Norris, J.P., Matilsky, T.A., 1989, *ApJ*, 346, 912
- Papadakis, I.E., Lawrence, A., 1993, *Nat.*, 361, 233
- Papadakis, I.E., Lawrence, A., 1995, *MNRAS*, 272, 161
- Papoulis, A.P., 1984, *Probability, Random Variables and Stochastic Processes*, McGraw-Hill, Singapore, 2nd ed.
- Pounds, K.A., Nandra, K., Stewart, G.C., Goerge, I.M., Fabian, A.C., 1990, *Nat.*, 344, 132
- Provenzale, A., Smith, L.A., Vio, R., Murante, G., 1992, *Physica*, D58, 31
- Provenzale, A., Vio, R., Cristiani, S., 1994, *ApJ*, 428, 591
- Schuster H.G., 1989, *Deterministic Chaos 2nd Ed.*, VCH, Weinheim
- Stern, B.E., Putanen, J., Svensson, R., Sikora, M., Begelman, M.C., 1995, *ApJ*, 449, L13
- Sugihara, G., May, R., 1990, *Nat.*, 344, 734
- Theiler, J., Galdrikian, B., Longtin, A., Eubank, S., Farmer, J.D., 1992, in *Nonlinear Modeling and Forecasting*, eds. M. Casdali and S. Eubank, (California: Addison Wesley), p. 163
- Tsonis, A.A., Elsner, J.B., 1992, *Nat.*, 358, 217
- Voges, W., Atmanspacher, H., Scheingraber, H., 1987, *ApJ*, 320, 794
- Walter, R., Fink, H.H., 1993, *A&A*, 274, 105
- Wandel, A., Liang, E.P., 1991, *ApJ*, 380, 84
- Wilkes, B.J., Elvis, M., 1987, *ApJ*, 323, 243
- Witt, H.J., Czerny, B., Życki, P.T., 1995, submitted to *MNRAS*
- Zdziarski, A.A., Johnson, W.N., Done, C., Smith, D., McNaron-Brown, K., 1995, *ApJ*, 438, L63
- Życki, P.T., Collin-Souffrin, S., Czerny, B., 1995, *MNRAS*, 277, 70
- Życki, P.T., Krolik, J., Zdziarski, A.A., Kallman, T.R., 1994, *ApJ*, 437, 597

APPENDIX A: DATA REQUIREMENTS

Nonlinear prediction method can be used to study the decay of short term correlations in the data and to discriminate whether X-ray emission is due to global but highly nonlinear behaviour of the emission region or due to multiple flares.

The presence of noise, however, limits the possibility to determine the type of behaviour. The error of prediction consists of both the error intrinsic to the dynamical character of the system and the statistical error given as a signal to noise ratio S/N .

The intrinsic error can again be characterized by the rate of decay of correlations, $(1 - R(T))^{1/2}$ and depends on the decay law (power law or exponential). The maximum time step of prediction is therefore limited by the condition

$$[1 - R(T)] + (N/S)^2 = 1. \quad (A1)$$

It means that the data allow to study the correlations up to

$$T = \frac{1}{2K} \ln \left[\frac{1}{A^2} (1 - (N/S)^2) \right] \quad (A2)$$

for exponential decay of correlation and

$$T = \left[\frac{1}{B} (1 - (N/S)^2) \right]^{\frac{1}{2H}} \quad (A3)$$

for power law decay of correlations. Here N/S stands for noise to signal ratio and A , B , H and K characterize the intrinsic source properties. These two formulae allow to estimate the improvement of the data quality with an increase of the signal to noise ratio.

This paper has been produced using the Blackwell Scientific Publications \TeX macros.